International Journal of Heat and Mass Transfer 130 (2019) 960–967

Contents lists available at ScienceDirect

International Journal of Heat and Mass Transfer

journal homepage: www.elsevier.com/locate/ijhmt

Evaluation of one-dimensional freezing behavior for ice-rich sandy soil

Gyu Hyun Go [a], Jangguen Lee [b,*], Hyu Soung Shin [b], Byung Hyun Ryu [b], Hyun Woo Jin [c], Deuk Woo Kim [d]

[a] Department of Civil Engineering, Kumoh National Institute of Technology, Gumi, Gyeongbuk 39177, Republic of Korea
[b] Department of Future Technology and Convergence Research, KICT, Goyang 10223, Republic of Korea
[c] Smart City & Construction Engineering, UST, Goyang 10223, Republic of Korea
[d] Department of Living and Built Environment Research, KICT, Goyang 10223, Republic of Korea

ARTICLE INFO

Article history:
Received 23 March 2018
Received in revised form 29 October 2018
Accepted 3 November 2018

Keywords:
Ice-rich sandy soil
1-D freezing
Phase change
Numerical analysis
Nonlinear regression

ABSTRACT

This paper evaluates a methodology that enables one-dimensional freezing to make a homogeneous frozen soil specimen. Numerical analyses that simulate one-dimensional freezing are conducted, considering the phase change of pore water. After evaluating the applicability of the numerical analysis model, the effects of geotechnical characteristics on the freezing behavior of ice-rich sandy soil are evaluated through parametric studies. In addition, a nonlinear regression model is proposed that can predict the time required for complete freezing of saturated soil. According to the results from nonlinear regression analysis, the model demonstrates reliable accuracy (R^2 = 0.998) in predicting the amount of time required for complete freezing, even with data from testing datasets not used in the developing stage.

1. Introduction

Due to continued population growth, sea level rise, and desertification, interest in the development of the Polar Regions is growing. The result is an increasing number of engineering activities in permafrost areas in response to the need for construction-infrastructure in Polar Regions. In particular, the importance of research and development on permafrost is being highlighted, and there have been extensive studies on the frozen soils in permafrost areas, based on experimental or theoretical approaches. For example, Mizoguchi [1] performed one-dimensional freezing tests for Kanagawa sandy loam, and evaluated the variation of volumetric water content with height during the freezing. Other researchers [2] established a macro kinetic model of ice crystal growth and verified it by the experimental and numerical simulation data [1,3]. Wu et al. [4] conducted indoor tests to examine the effects of solutes on soil freezing, and they found that the solute content and solute type had significant influences on soil-freezing characteristics. Zhang el al. [5] studied pore water pressure and the consolidation phenomenon in unfrozen zone during soil freezing. They concluded that the changes in the pore water pressure in the unfrozen zone are mainly controlled by the stress and hydraulic boundary conditions at the freezing point. Fukuda et al. [6] conducted one-dimensional freezing tests with varying the way of freezing: step freezing and ramped freezing, and they evaluated the amounts of frost heave for each testing method. Yurui et al. [7] conducted a series of triaxial compression tests on frozen silt specimens, and established a new strength criterion for frozen soil. The new strength criterion has nonlinear characteristics on meridian and deviatoric planes, which could reflect pressure sensitivity and an effect from principal direction. Lai et al. [8] established a phase change kinetic model for saline soil, and found that the macroscopic crystallization stress generated by phase change contributed to the soil deformation. More recently, Wang et al. [9] investigated the freezing-induced moisture redistribution in fine-grained soil under high pressure.

In most of the previous research, the physico-mechanical properties of ice-rich soils have been investigated with undisturbed and remolded frozen soil specimens. Although it is recommended to explore the physical properties of ice-rich soils using undisturbed specimens, much of the fundamental research is still being conducted with specimens artificially prepared in the laboratory. In general, there are two basic freezing methods: multiaxial and uniaxial [10]. The multi-axial freezing method causes a specimen to freeze on all exposed surfaces at the same time. It is used to prepare specimens for testing related to artificial ground freezing. However, it is hard to obtain uniform moisture distribution through the test specimen. The uniaxial freezing method is used to freeze a specimen only from the top, during which free water is supplied from the bottom of the specimen. The water level is kept even with the top of the specimen, which allows it to expel or take water in during freezing so that uniform moisture distribution can be achieved. Around surfaces are

* Corresponding author.
E-mail address: jlee@kict.re.kr (J. Lee).

https://doi.org/10.1016/j.ijheatmasstransfer.2018.11.017
0017-9310/

Table 1
Freezing rates for test specimens with 69 mm diameter and 140 mm [13,14].

Type	Freezing rate	
	mm/day	%/day
Distilled water	6	4.3
Ottawa sand	38	27.1
Manchester fine sand	40	28.6
Hanover silt	80	57.1
Suffield clay	170	121.4

insulated using granulated cork or vermiculite [11,12]. Several researchers have found that rapid uniaxial freezing causes air to be trapped in a specimen. Thus, typical freezing rates were proposed, and are presented in Table 1 [13,14]. The freezing rate is defined as the rate of progress of the 0 °C (32 °F) isotherm, which is normally determined by means of thermocouples installed through the center of the specimen [13]. In this regard, an accurate evaluation of soil thermal properties is needed to determine the appropriate freezing rate of a test specimen. Although many studies have dealt with evaluation of thermal properties of frozen soil, most of them were focused on estimating thermal conductivity [15–25]. However, it is experimentally tedious to utilize a freezing rate that mainly depends on the thermal conductivity of a tested soil specimen. Even if the soil classifications of different samples are similar, their thermal characteristics may vary depending on the mineral components, dry density, volumetric fraction of soil void, and pore-water. In addition, the thermal regime in cold regions is strongly affected by freezing processes, which release large amounts of latent heat [26]. Hence, in-depth studies and discussions about freezing processes are needed that consider the phase changes of pore-water. Therefore, the aim of this study was to evaluate the thermal characteristics of ice-rich sandy soils when one-dimensional (1-D) freezing is applied. In order to do this, finite element analyses were conducted for simulations of the 1-D freezing behavior of ice-rich soil, with consideration of the phase changes of pore-water. Furthermore, the model was able to evaluate the effect of geotechnical characteristics on the freezing behavior of saturated soil, and a nonlinear regression model was finally proposed that can predict the time required for complete freezing of saturated soil.

2. Experimental setup

For precise geotechnical testing in ice-rich soils, a method of making specimens is required to ensure that the water inside voids is homogeneously frozen. To do this, it is necessary to have a methodology that enables 1-D freezing of water because the freezing behavior of ice-rich soils is mainly governed by that of pore-water. Thus, 1-D water-freezing tests were performed. A small freezing box (25 × 25 × 18 cm; 2.5 cm thick) was made from dense polystyrene. A cooling-plate 2.0 cm thick was placed on the bottom of the freezing box and constant low temperature was maintained by passing a freeze-resistant liquid through the cooling plate. Thermocouples were installed 2 cm apart along the vertical axis at the center of the freezing box, and then distilled water was poured to a depth of 14 cm and carefully stirred to remove entrapped air. A polystyrene plate (2.5 cm thick) covered the freezing box and was sealed tightly. An empty space (2 cm) above the water level accommodated volumetric expansion caused by changes in the water–ice phase during freezing.

3. Numerical simulation

3.1. Heat conduction in porous media

In this study, a commercial Finite Element (FE) code COMSOL Multi-Physics [27] was adopted to evaluate the thermal behavior of saturated soil during the freezing process. The FE model that solves the heat transfer problems considering the phase change of pore-water was based on following basic assumptions:

1. The void of the material exists in a saturated state without air. In the frozen state, the void consists of ice and unfrozen water, in the non-frozen state, the void is completely saturated with water.
2. The materials are considered as a sandy soil, which is not susceptible to frost heaving: we assumed that frost heaving does not occur during the freezing in the soil.
3. The materials consisting of three phases of soil particles, water, and ice have the same temperature at the same point in the local temperature equilibrium condition.
4. The heat transfer in the porous medium only occurs by conduction.

Thus, the governing equation of the heat conduction could be expressed as follows [28]:

$$\rho \frac{\partial h(T)}{\partial t} - \nabla \cdot (k \nabla T) = 0 \tag{1}$$

where $h(T)$ is the specific enthalpy ($J \cdot kg^{-1}$), ρ is the equivalent density ($kg \cdot m^{-3}$), and k is the equivalent thermal conductivity ($W \cdot m^{-1} \cdot K^{-1}$) of a porous medium. By applying the chain rule to the time derivative term, Eq. (1) becomes:

$$\rho \frac{\partial h}{\partial T} \frac{\partial T}{\partial t} - \nabla \cdot (k \nabla T) = 0 \tag{2}$$

where the term $\partial h/\partial T$ represents the derivative of enthalpy with respect to temperature, which is equivalent to the specific heat capacity C_p ($J \cdot kg^{-1} \cdot K^{-1}$) of porous media. Thus, the heat conduction equation can be rewritten as follows:

$$\rho C_p \frac{\partial T}{\partial t} - \nabla \cdot (k \nabla T) = 0 \tag{3}$$

Here, the equivalent thermal properties can be expressed in compliance with the volume fraction.

$$\begin{aligned} k &= k_s(1-\Phi) + k_v \Phi \\ \rho &= \rho_s(1-\Phi) + \rho_v \Phi \\ C_p &= C_{p,s}(1-\Phi) + C_{p,v}\Phi \end{aligned} \tag{4}$$

where Φ is the volume fraction of the pore space, commonly called the porosity. Thus, 1-Φ is the solid volume fraction. The subscript s and v of each parameter refers to solid and void, respectively.

3.2. Phase change of water

Based on the heat conduction equation presented in Eq. (3), the freezing of water can be considered by quantifying the change of thermal properties such as density, thermal conductivity, and specific heat. When the temperature drops below the freezing point (T_{fp} = 273.15 K for water), part of the water in the pore space changes to ice, leading to a drop in the density and a rise in the thermal conductivity. The concept of apparent heat capacity was invoked to allow consideration of the latent heat associated with freezing [29].

$$\begin{aligned} k_v &= k_{water}\Theta + k_{ice}(1-\Theta) \\ \rho_v &= \rho_{water}\Theta + \rho_{ice}(1-\Theta) \\ C_{p,v} &= \frac{1}{\rho_v}(\rho_{water} \cdot C_{p,water}\Theta + \rho_{ice} \cdot C_{p,ice}(1-\Theta)) + (h_{ice} - h_{water})\frac{\partial \alpha_m}{\partial T} \end{aligned} \tag{5}$$

where h_{ice} and h_{water} is specific enthalpy ($J \cdot kg^{-1}$) of ice and water, respectively. Because of complicated processes in a porous medium,

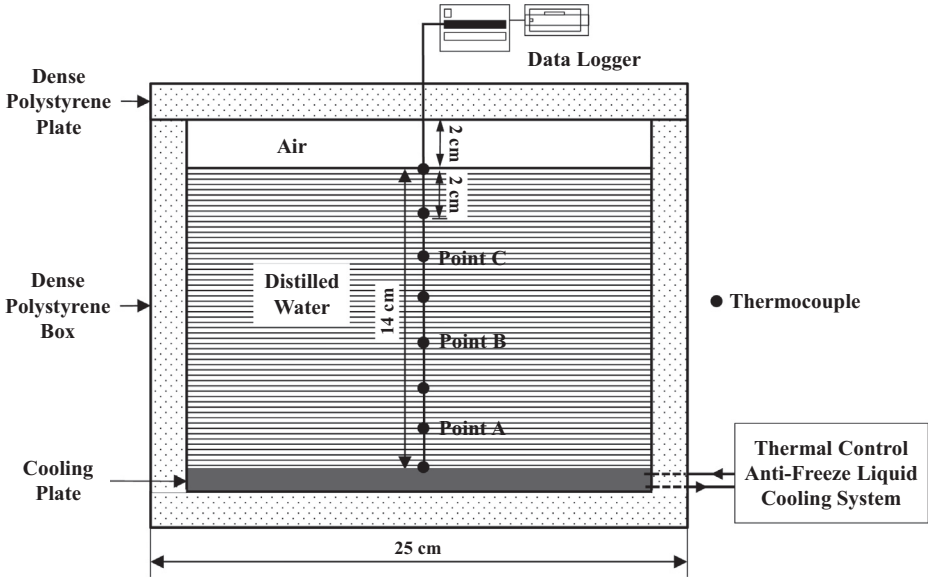

Fig. 1. Schematic diagram of experimental setup.

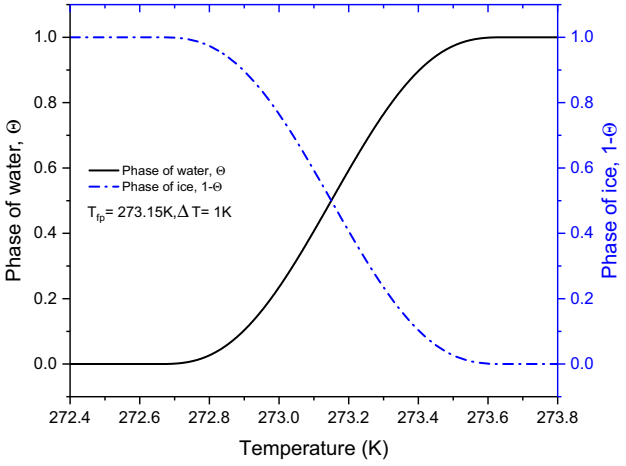

Fig. 2. Heaviside functions that represent the liquid and solid phases of water.

freezing cannot be considered a simple discontinuity. Thus, the Heaviside function is generally assumed to be a continuous function of temperature within a specified interval [30]. Here, the Heaviside function, Θ, represents the phase of water, which varies from '1' to '0'. At the freezing point, the phase of ice, $1-\Theta$, varies inversely (Fig. 2). In addition, $\partial\alpha_m/\partial T$ is the Dirac pulse that occurs in a temperature interval between $(T_{fp}+\triangle T/2)$ and $(T_{fp}-\triangle T/2)$; hence, $(h_{ice}-h_{water})\,\partial\alpha_m/\partial T$ represents the distribution of latent heat ($J{\cdot}kg^{-1}{\cdot}K^{-1}$). The mass fraction α_m can be defined in compliance with Θ as follows:

$$\alpha_m = \frac{1}{2}\frac{(1-\Theta)\rho_{ice}-\Theta\rho_{water}}{\rho_v} \tag{6}$$

3.3. Boundary conditions of the finite element model

As shown in Fig. 3, the governing equation for heat conduction was applied in all domains, and the heat flow q was calculated according to Fourier's law of heat conduction. The initial temperature of the specimen, $T_0 = 20\,^{\circ}C$, was defined in whole domains, and the bottom temperature was fixed at $-10\,^{\circ}C$. Because the air space remained on the top to accommodate volume expansion in

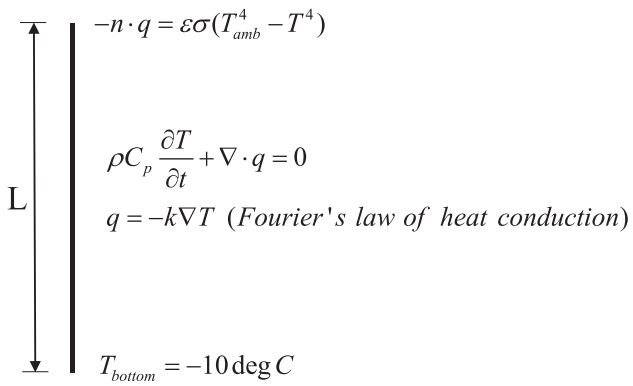

Fig. 3. Boundary condition of the finite element model.

the experiment, a 'Diffuse surface' condition was also defined at the top boundary. Here, the surface emissivity of ice used, was 0.97 [31,32].

4. Results and discussion

4.1. Model verification

The material properties used in the model are presented in Table 2, and the boundary conditions are shown in Fig. 3. Fig. 4 shows the results of the FE analyses that simulates the freezing behavior of water. The dashed lines represent the distributions of latent heat at the top and Point B in Fig. 1. During the phase change of water at the top, heat sink energy is released by the phase change instead of creating a temperature drop. The time of the phase change depends on a duration at which the Dirac pulse $(\partial\alpha_m/\partial T)$ is generated. If the observation point gets closer to the bottom where a heat sink is located, the duration of the latent heat distribution would become short and the time of phase change would also be shorter. To evaluate the reliability of the FE model, the prediction results were verified by comparison with measurements from the experiment. As shown in Fig. 5, the results of the FE model showed fairly good agreement with the measured data. Once the reliability of the predictions for the behavior of freezing water has been verified, the model could be extended to porous

Table 2
Material properties used in the numerical simulation model.

Material properties	Value	Unit
Density of water, ρ_{water}	997	kg·m^{-3}
Density of ice, ρ_{ice}	918	kg·m^{-3}
Heat capacity of water at constant pressure	4179	J·kg^{-1}·K^{-1}
Heat capacity of ice at constant pressure	2052	J·kg^{-1}·K^{-1}
Thermal conductivity of water, k_{water}	0.613	W·m^{-1}·K^{-1}
Thermal conductivity of ice, k_{ice}	2.31	W·m^{-1}·K^{-1}
Latent heat of fusion, l_m	333.5	kJ·kg

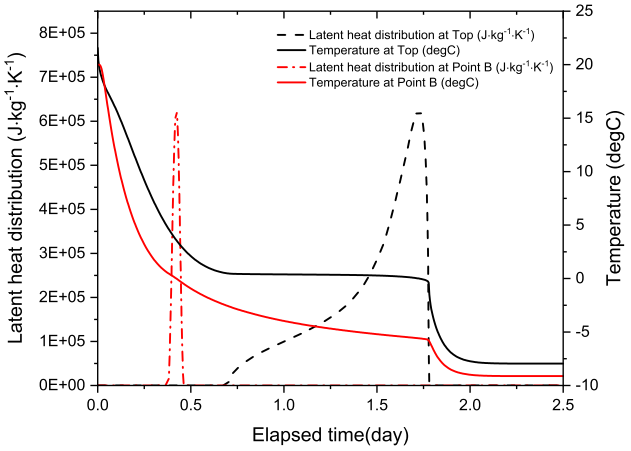

Fig. 4. Finite element analysis results for simulating the process of freezing water.

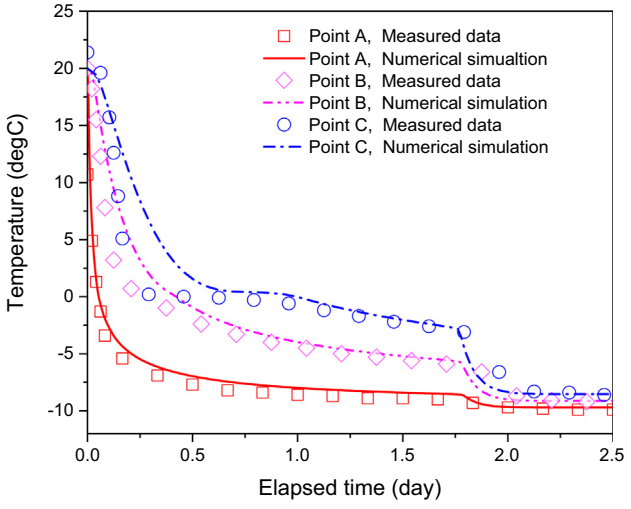

Fig. 5. Comparison of temperature variation by measured data and numerical simulation.

media using the volume average relationship presented in Eq. (4). Fig. 6 shows the comparison of results for the freezing curves of water and saturated soil. When compared to a water sample under the same conditions, fully saturated soil exhibits a sudden temperature drop until it reaches the freezing point, and the time at which a phase change occurs is significantly reduced. However, these differences vary with geotechnical properties (e.g., thermal conductivity of soil particles and porosity).

4.2. Effect of geotechnical characteristics

To examine the effect of geotechnical characteristics on the freezing behavior of saturated soil, parametric studies were conducted with respect to the key factors. The parameters and the ranges considered are presented in Table 3, and the height of the specimens was set to 140 mm. Through the results of parametric studies, it was clearly confirmed that the thermal conductivity of the soil particles and the porosity have great effects on the freezing behavior of saturated soil (Fig. 7). As the thermal conductivity of the soil particles increases and the porosity decreases, the freezing becomes faster and the progression of phase change is accelerated. This means that the freezing behavior of saturated soil is more affected by the soil particles than by the energy release from phase change, if the thermal conductivity of the soil particles increases. Moreover, the loss of heat sink energy by surface emission was least when the thermal conductivity of the soil particles was highest. If the thermal conductivity of the soil particles is too low, the heat sink energy from the bottom is not easily transferred to the top; hence, the effect of surface emission at the top also increases.

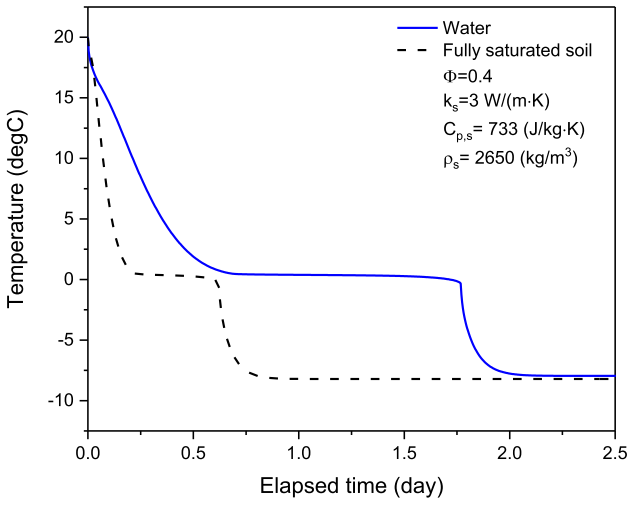

Fig. 6. Comparison of the freezing curves of water and fully saturated soil.

4.3. Time required for complete freezing

Fig. 8 shows the degree of freezing (%) with time. Herein, the degree of freezing was considered to be the frozen height compared to the entire height of specimen, and freezing was defined as the moment when the phase change was terminated and the temperature dropped below 0 °C. That is, 100% degree of freezing means that the 0 °C isotherm reaches the top of the specimen. As shown in Fig. 8, as the thermal conductivity of the soil particles increases, and the porosity decreases, the time to reach complete freezing shortens. When the thermal conductivity of the soil particles increased 1.5 times (comparing specimens with the same porosity), the time to reach complete freezing decreased about 0.75 times. When the porosity increased 1.5 times (comparing two samples with the same soil-particle thermal conductivity), the time to reach complete freezing increased about 1.5 times. That is, the porosity tends to be proportional to the freezing time, and the thermal conductivity of the soil particle tends to be inversely proportional to the freezing time. Fig. 9 is a contour plot of the time required for complete freezing according to the porosity and the

Table 3
Key parameters and range.

Parameters	Value	Unit
Porosity, Φ	0.30, 0.35, 0.40, 0.45	
Soil particle thermal conductivity, k_s	2.0, 3.0, 4.0, 5.0	W·m^{-1}·K^{-1}

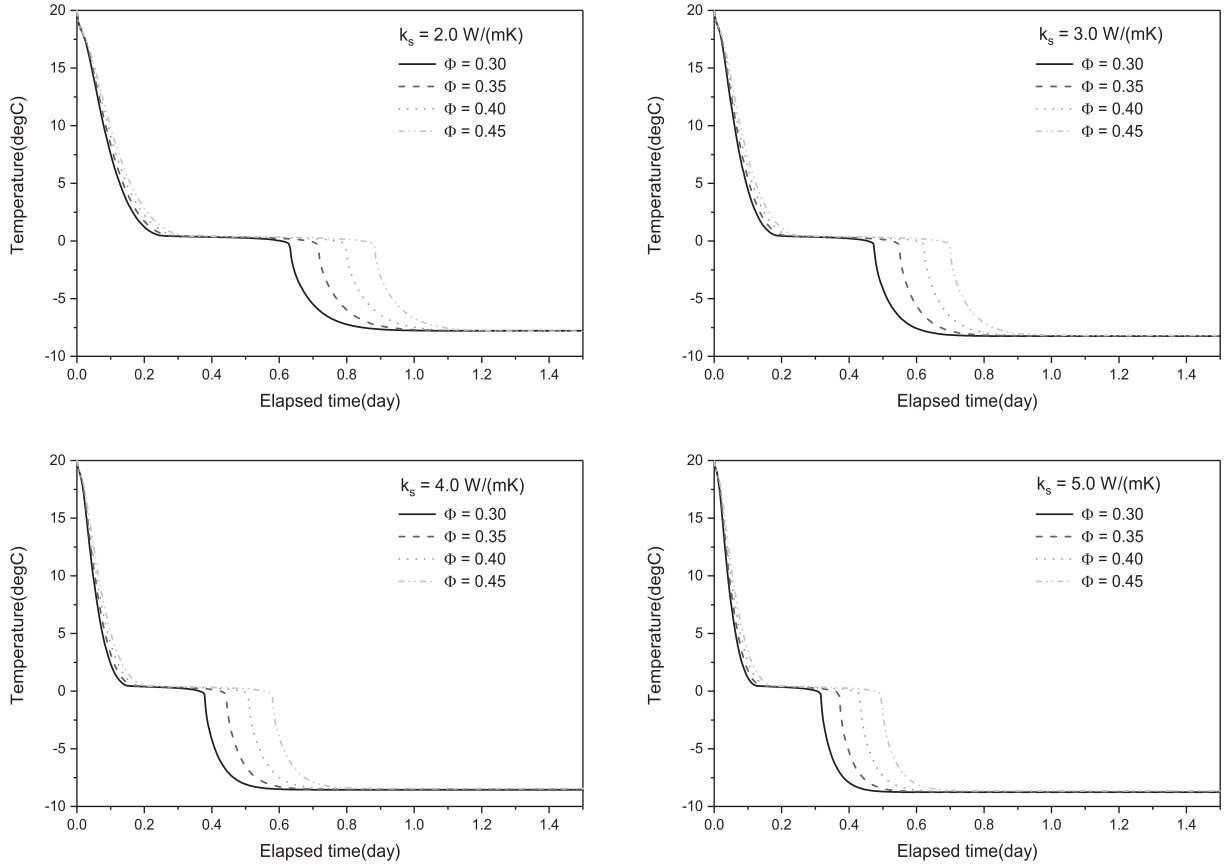

Fig. 7. Effect of geotechnical properties on the freezing curve of saturated soil.

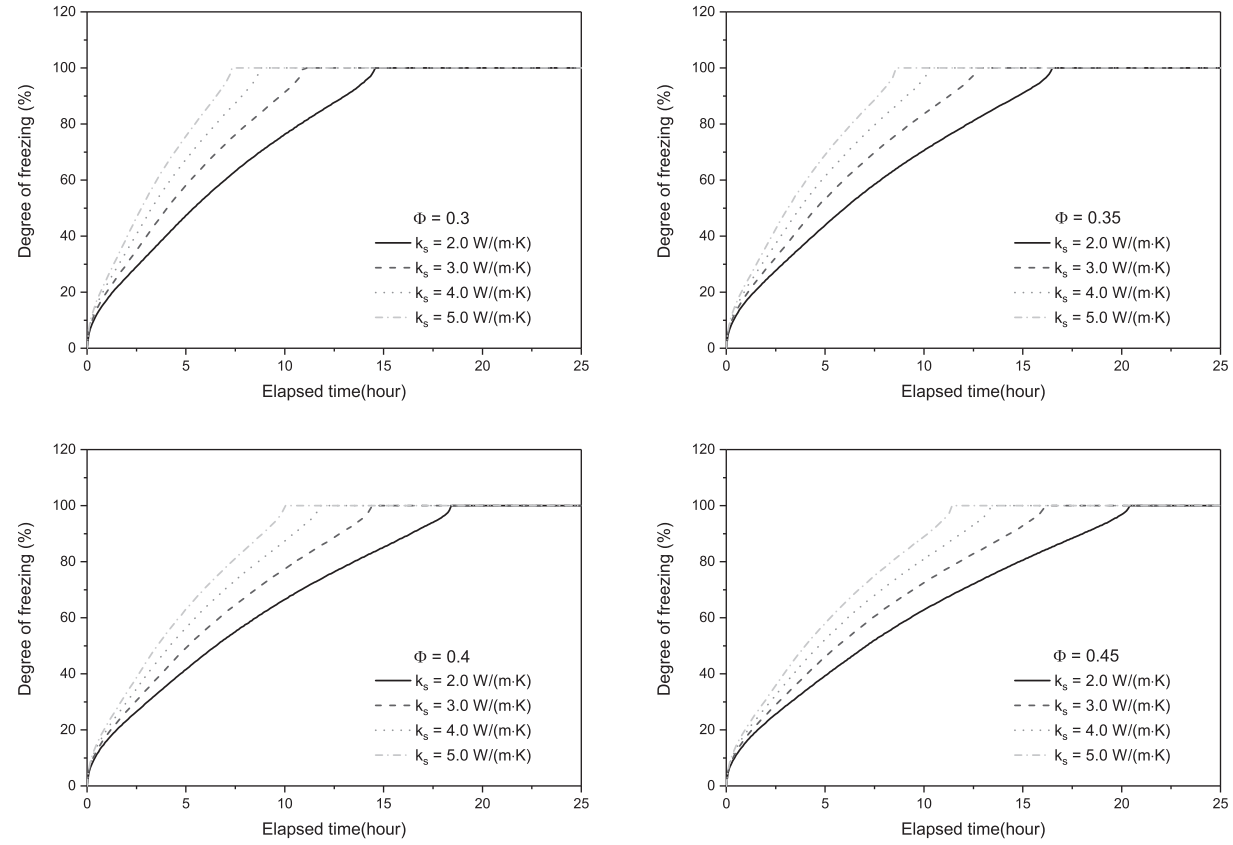

Fig. 8. Effect of geotechnical properties on the degree of freezing.

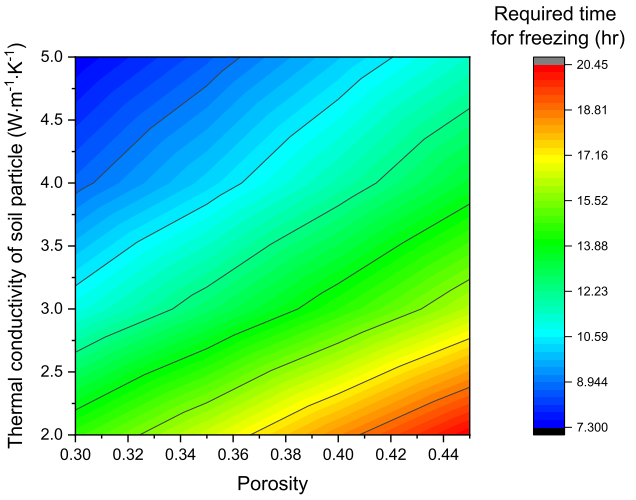

Fig. 9. Effect of geotechnical properties on the time required for fully freezing.

thermal conductivity of the soil particles. It was confirmed that the time required for freezing becomes more sensitive to the soil particle thermal conductivity as the porosity increases.

In addition, the time required for freezing is also greatly influenced by the specimen height. Fig. 10 shows the amount of time required for complete freezing according to the height of the specimen. For example, when soils having a particle thermal conductivity of 2.0 $W{\cdot}m^{-1}K^{-1}$ are formed in a 140 mm-height soil specimen with a porosity of 0.45, the amount of time required for complete freezing will take about 1225 min. This will help to set the operating period of the cooling system at an early stage. However, these results may vary with the freezing rate, which is determined by temperature conditions and specimen height.

Also, as the height of the specimen increases, the time required for complete freezing exponentially increases. Moreover, the larger the porosity of the soil specimen is, the greater the increase in freezing time. This is because the larger the porosity is, the greater the freezing delay effect due to phase change of water in the void.

4.4. Nonlinear regression analysis

As shown in Figs. 7–9, the amount of complete freezing time of the saturated soil was positively correlated with the porosity (Φ), and negatively correlated with thermal conductivity of soil particle (k_s). In addition, there was a positive correlation with the height of the specimen (H) (Fig. 10). Therefore, a stepwise regression analysis was conducted considering a 'polynomial model' because the amount of freezing time had nonlinear relationships with the three influencing factors. The polynomial model contains an intercept, linear terms, all interactions, and squared terms for each predictor (Φ, k_s, H).

$$t_{fr} = b_0 + b_1 \cdot \Phi + b_2 \cdot k_s + b_3 \cdot H + b_4 \cdot \Phi \cdot k_s + b_5 \cdot \Phi \cdot H + b_6 \cdot k_s \cdot H + b_7 \cdot k_s^2 + b_8 \cdot H^2 \quad (7)$$

When constructing a regression model, if there are several independent variables that affect the dependent variable, it is important to select an independent variable with good explanatory power [33]. In general, stepwise regression analysis is used as the input variable selection method. Stepwise regression analysis is an iterative process in which the statistical significance is determined by adding or removing independent variables at each step, based on the probability of F (p-value). In this study, the p-value

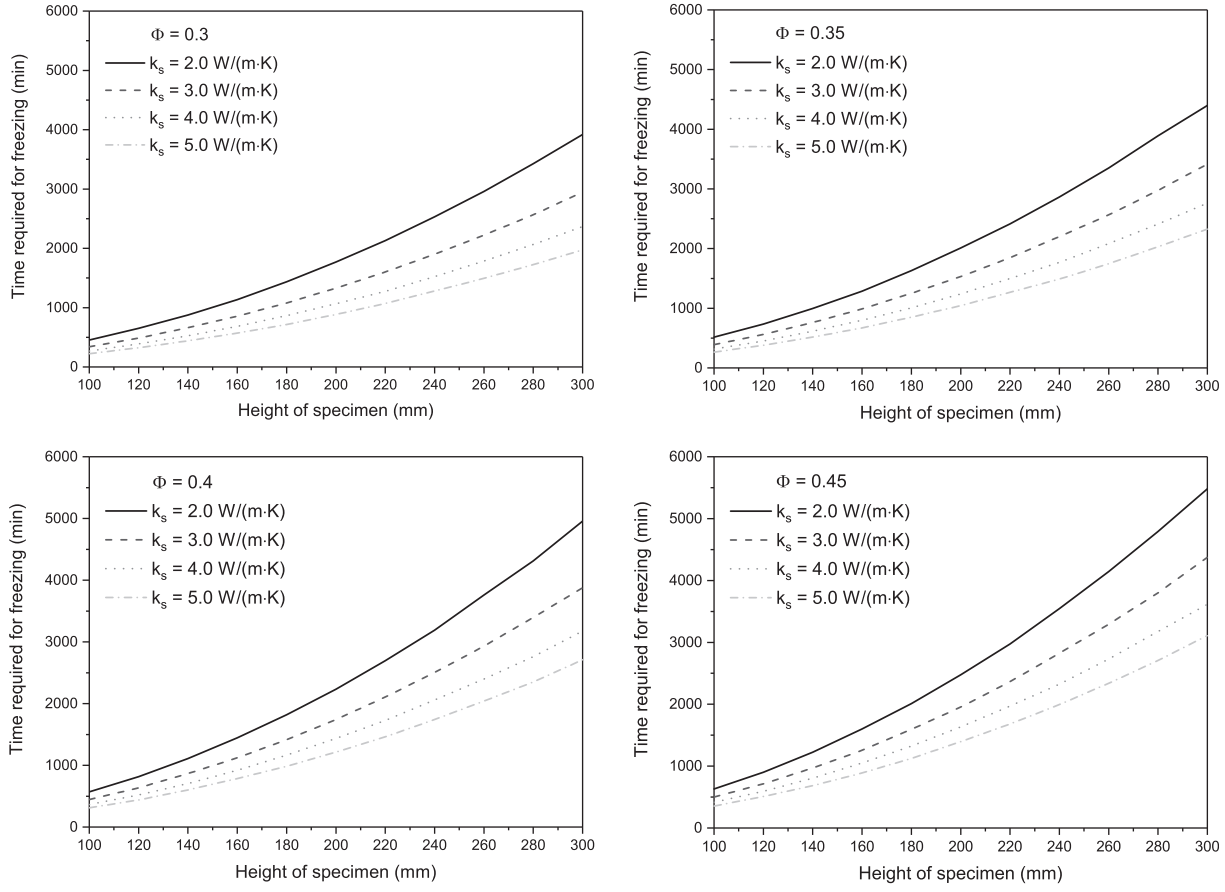

Fig. 10. Amount of time required for freezing according to the specimen height.

Table 4
Results of nonlinear regression analysis.

Parameter	Equation term	Estimated coefficients, b	Standard coefficient, β	p-Value	Remark
b_0	Intercept	598.40	−0.217	<0.0001	
b_1	Φ	−2160.02	0.214	<0.0000	
b_2	k_s	−59.56	−0.348	0.167	
b_3	H	−3.31	0.853	<0.0000	The most influential factor
b_4	$\Phi \cdot k_s$	−372.28	−0.021	<0.0000	
b_5	$\Phi \cdot H$	38.75	0.123	<0.0000	
b_6	$k_s \cdot H$	−3.27	−0.207	<0.0000	
b_7	k_s^2	72.05	0.081	<0.0000	
b_8	H^2	0.04	0.137	<0.0000	

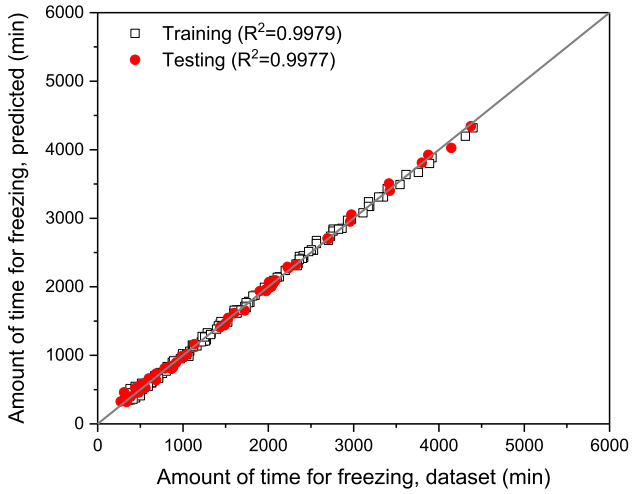

Fig. 11. Prediction results of the regression model (training set and validation set cases).

criterion for adding and removing of independent variables was set to 0.05 and 0.1, respectively. A regression model was constructed by randomly extracting 123 of 176 samples; the remaining 53 samples were used to verify the model.

Table 4 shows the final results of the stepwise regression analysis. The adjusted coefficient of determination ($_{adj}R^2$) in the developed model was 0.9979 (Fig. 11). The model reasonably explained the relationship between three independent variables and dependent variables (the RMSE (Root Mean Square Error) was 46.28 min). Moreover, from the standard beta coefficients in Table 4, it is confirmed that the height of a specimen has the greatest impact on the dependent variable (positively correlated), and the next most influential parameter is the particle thermal conductivity (negatively correlated). The porosity has the smallest impact on the dependent variable (positively correlated). To evaluate the applicability of the regression model, it was tested with 53 data sets that had not been used in the development stage, and the verification results showed that it had high accuracy (RMSE is 52.10 min) even for testing. These results imply that the proposed regression model is reliable for predicting the amount of time for complete freezing of saturated soil, and is applicable to set the operating period of the cooling system at an early stage.

5. Summary and conclusions

In this study, numerical analyses were conducted to evaluate freezing behavior in ice-rich sandy soil considering the phase change of pore-water. To evaluate the reliability of the FE model, the prediction results were verified by comparison with those measured from the experiment, and the FE model showed reliable prediction results for 1-D freezing tests of water. After verifying the accuracy of the model for the freezing behavior of water, the model was extended to a porous medium and used to evaluate the effect of geotechnical characteristics on the freezing behavior of saturated soil. The main conclusions drawn from the study results are summarized below.

1. When compared to a water specimen, saturated soil exhibited a sudden temperature drop until it reached the freezing point, and the time at which the phase change occurs was significantly reduced. However, these differences are dependent on various geotechnical properties such as the particle thermal conductivity and the porosity.
2. The freezing behavior of saturated soil is more affected by the soil particles than by the energy release by phase change, if the thermal conductivity of soil particles is high. Whereas, if the thermal conductivity of the soil particles is low, the heat sink energy from the bottom is not easily transferred to the top, and the impact of surface emission increases.
3. The porosity is linearly proportional to the freezing time, while the thermal conductivity of the soil particles is non-linearly and inversely proportional to the freezing time. In addition, the height of a specimen has a great influence on the time required for freezing. As the specimen height increases, the time required for complete freezing increases exponentially. Moreover, the larger the porosity of the specimen, the greater the increase in the freezing time.
4. The nonlinear regression model demonstrated reliable accuracy (R^2 = 0.9979) in predicting the amount of time required for complete freezing for 123 simulated data, and showed excellent agreement with additional 53 testing data that had not been used in the development stage. In addition, the estimated standard coefficients in the regression analysis indicated that the height of a specimen had the greatest impact on the dependent variable. The second most influential parameter was the particle thermal conductivity, and the porosity had the smallest impact on the dependent variable. The proposed model will be useful not only for the preparation of frozen specimens, but also for setting the operating period of the cooling system at an early stage.

Conflict of interest

The authors declared that there is no conflict of interest.

Acknowledgements

This research was supported by the research project "Development of environmental simulator and advanced construction technologies over TRL6 in extreme conditions" funded by KICT.

References

[1] M. Mizoguchi, Water Heat and Salt Transport in Freezing Soil PhD thesis, University of Tokyo, Tokyo, 1990.
[2] D. Wu, Y. Lai, M. Zhang, Heat and mass transfer effects of ice growth mechanisms in a fully saturated soil, Int. J. Heat Mass Trans. 86 (2015) 699–709.
[3] K. Hansson, J. Simunek, M. Mizoguchi, L.C. Lundin, M.T. van Genuchten, Water flow and heat transport in frozen soil: numerical solution and freeze–thaw applications, Vadoze Zone J. 3 (2) (2004) 693–704.
[4] M. Wu, X. Tan, J. Huang, J. Wu, P.E. Jansson, Solute and water effects on soil freezing characteristics based on laboratory experiments, Cold Regions Sci. Tech. 115 (2015) 22–29.
[5] L. Zhang, W. Ma, C. Yang, Z. Wen, S. Dong, An investigation of pore water pressure and consolidation phenomenon in the unfrozen zone during soil freezing, Cold Regions Sci. Tech. 130 (2016) 21–32.
[6] M. Fukuda, H. Kim, Y. Kim, Preliminary results of frost heave experiments using standard test sample provided by TC8, in: Proceedings of the International Symposium on Ground Freezing and Frost Action in Soils, Lulea, Sweden, 1997, pp. 25–30.
[7] Y. Yugui, G. Feng, C. Hongmei, H. Peng, Energy dissipation and failure criterion of artificial frozen soil, Cold Regions Sci. Tech. 129 (2016) 137–144.
[8] Y. Lai, D. Wu, M. Zhang, Crystallization deformation of a saline soil during freezing and thawing processes, Appl. Therm. Eng. 120 (2017) 463–473.
[9] D. Wang, Y. Wang, W. Ma, L. Lei, Z. Wen, Study on the freezing-induced soil moisture redistribution under the applied high pressure, Cold Regions Sci. Tech. 145 (2018) 135–141.
[10] O. Andersland, B. Ladanyi, An Introduction to Frozen Ground Engineering, first ed., Wiley and Sons, Hoboken, NJ, 1994.
[11] T.H.W. Baker, Transport, preparation and storage of frozen soil samples for laboratory testing, Soil Specimen Preparation for Laboratory Testing, ASTM Spec. Tech. Pub. 599 (1976) 88–112.
[12] V.R. Parameswaran, S.J. Jones, Triaxial testing of frozen sand, J. Glaciol. 27 (95) (1981) 147–155.
[13] F.H. Sayles, Creep of frozen sands, U.S. Army Cold Region Research and Engineering Laboratory, Technical Report No. 190, 1968.
[14] F.H. Sayles, D. Haines, Creep of Frozen Silt and Clay, U.S. Army Cold Region Research and Engineering Laboratory, Technical Report No. 252, 1974.
[15] M.S. Kersten, Laboratory research for the determination of the thermal properties of soils, Research Laboratory Investigations, Engineering Experiment Station, University of Minnesota, Minneapolis, Minn. Technical Report 23, 1949.
[16] O. Johansen, Thermal conductivity of soils. PhD thesis, University of Trondheim, Trondheim, Norway, US Army Corps of Engineers, Cold Regions Research and Engineering Laboratory, Hanover, N.H. CRREL Draft English Translation 637, 1975.
[17] J. Côté, J.M. Konrad, Thermal conductivity of basecourse materials, Can. Geotech J. 42 (2005) 61–78.
[18] D.M. Anderson, A.R. Tice, Predicting unfrozen water content in frozen soils from surface area measurements, National Research Council, Washington, D.C. Highway Research Record No. 393, 1972, pp. 12–18.
[19] O.T. Farouki, Thermal properties of soils, US Army Corps of Engineers, Cold Regions Research and Engineering Laboratory, Hanover, N.H. CRREL Monograph 81-1, 1981.
[20] E. Penner, Thermal conductivity of frozen soils, Can. J. Earth Sci. 7 (1970) 982–987.
[21] F. Gori, New model to evaluate the effective thermal conductivity of three-phase soils, Int. Commun. Heat Mass Trans. 47 (2013) 1–6.
[22] S. Negrelli, R.P. Cardoso, C.J.L. Hermes, A finite-volume diffusion-limited aggregation model for predicting the effective thermal conductivity of frost, Int. J. Heat Mass Trans. 101 (2016) 1263–1272.
[23] W.A. Slusarchuk, G.H. Watson, Thermal conductivity of some ice-rich permafrost soils, Can. Geotech. J. 12 (3) (1975) 413–424.
[24] V. Balland, P.A. Arp, Modeling soil thermal conductivities over a wide range of conditions, J. Environ. Eng. Sci. 4 (6) (2005) 549–558.
[25] B.R. Becker, A. Misra, B.A. Fricke, Development of correlations for soil thermal conductivity, Int. Commun. Heat Mass Trans. 19 (1992) 59–68.
[26] D. Mottaghy, V. Rath, Latent heat effects in subsurface heat transport modelling and their impact on palaeotemperature reconstructions, Geophys. J. Int. 164 (2006) 236–245.
[27] Comsol Inc., Comsol multiphysics user's manual Ver. 5.4, USA, 2018.
[28] F.P. Incropera, D.P. Dewitt, Fundamentals of Heat and Mass Transfer, fifth ed., John Wiley & Sons Inc., NY, USA, 2002, p. 981.
[29] I.T. Kukkonen, J. Safanda, Numerical modelling of permafrost in bedrock in northern Fennoscandia during the Holocene, Glob. Planet. Change 29 (2001) 259–273.
[30] V.J. Lunardini, Freezing of soil with an unfrozen water content and variable thermal properties, CRREL report 88-2, Nat. Tech. Info. Serv., 88-2, 23, 1987.
[31] M.Q. Brewster, Thermal Radiative Transfer and Properties, John Wiley & Sons, 1992, p. 56. ISBN 9780471539827.
[32] 2009 ASHRAE Handbook: Fundamentals – IP Edition. Atlanta: American Society of Heating, Refrigerating and Air-Conditioning Engineers, 2009. ISBN 978-1-933742-56-4.
[33] N.R. Draper, H. Smith, Applied Regression Analysis, second ed., John Wiley & Sons Inc., NY, USA, 1998, pp. 307–312.